Chapter 3

ADSORPTION AND DIFFUSION OF CARBON ADATOMS —LDA Approaches

3.1 Introduction

More accurate calculations by the density functional theory are performed in this chapter. We concentrate on the behaviors of the carbon adatoms The diffusion processes of the carbon adatoms are discussed in detail. The LDA calculations of the NT have been already performed to investigate electronic [9, 83, 84, 85, 86, 87] and mechanical [82, 88] properties. For the growth mechanisms of the NT, there are several LDA calculations [59, 61, 62]. Charlier *et al.* have performed the molecular dynamics (MD) simulation for the open edge of the SWNT and the double wall NT by the LDA calculation. They have shown that the SWNT edge without the metal catalysts is spontaneously closed by a graphitic dome. On the other hand, they have also shown, in the case of the double wall NT, that the chemical bonding between the inner tube and the outer tube (the lip-lip interaction) [61] makes the edge of the double wall NT metastable, suggesting that the MWNT can grow without the metal catalyst. Lee *et al.* have shown that an activation barrier for diffusion of a Ni atom on the NT edge is less than that of the C atom [59] using the cluster code DMol [67]; the Ni atom diffusing on the NT edge assists in annealing out defects such as a pentagon which is responsible for the tube closure. Kwon *et al.* have calculated total energies of several edges of MWNTs with adatoms also using the DMol code and the parametrized linear combination of atomic orbitals method. They have shown that the edges of the MWNTs are stabilized against tube closure by interactions between the inner and outer tubes (the lip-lip interaction) [62].

In this chapter, we explore the stable or metastable adsorption sites for the carbon adatom on both the achiral armchair $(n,0)$-tube and zigzag $(n,0)$-tube edge. The activation energies of the adatom diffusion on the NT edge are also calculated. In addition to the adatom on the NT edge, the adatoms on the NT wall are considered. It is found that the adatoms on the NT wall also play an important role of the NT growth, since the adatoms on the wall diffusing toward the open edge

are probably incorporated into the NT honeycomb lattice at the edge. As mentioned above, several pentagons are likely to be formed on the NT edge during the open edge growth. The pentagons on the NT edge that promote the tube closure must be annealed out to maintain the open edge growth. The process of annealing out from the pentagon network to the hexagon network on the NT edge by incorporation of a single adatom into the pentagon is discussed. It is also found that the polygonal defects on the NT edge are annealed out by incorporation of the wall adatom with relatively small activation energies.

3.2 Methods of Calculations

All calculations in this chapter are performed by the density functional theory [89, 90] with the local-density approximation. The exchange-correlation energy is expressed by the Ceperley-Alder results [91] interpolated by Perdew and Zunger [92]. (The formulations of the density functional theory and the functional forms of the exchange-correlation energy for the unporalized homogeneous electron gas used in this thesis are given in Appendix A.) The core electrons are replaced by a norm-conserving pseudopotential (PP) constructed by the Troullier-Martins scheme [93]. Troullier and Martins have constructed the PP of the carbon atom with the core radii of 1.50 bohr for the $2s$ state and 1.54 bohr for the $2p$ state in their original paper [93]. Then, the total energies of the diamond have been calculated by the plane wave basis set with various cutoff energies $E_{\rm cut}$ up to 100 Ry. They have shown that the total energy converged within 0.1 eV at $E_{\rm cut}$=49 Ry [93]. The structural properties (the lattice constant and the bulk modulus) are calculated by the LDA calculations using the plane wave basis set with $E_{\rm cut}$=49 Ry. They have also shown that these results agreed with experimental results satisfactorily [93]. On the other hand, in this chapter, we set the core radii for both the carbon $2s$ and $2p$ states at 1.6 bohr to construct the more soft PP. We investigate this PP with the single graphite sheet. The total energies of the single graphite sheet converge within 0.3 eV at $E_{\rm cut}$=35 Ry. It is found that the lattice constant of the graphite obtained by the LDA calculations with $E_{\rm cut}$=35 Ry agrees with the experimental value within the error of 1.2 %. The computational time is saved by reduction of the cutoff energy of the plane wave basis set. Therefore, we use this PP for the LDA calculations in this thesis. (The construction scheme of the PP by Troullier and Martins is given in Appendix B.)

We use a supercell model. The unitcells prepared for the calculations are given in each following section. The conjugate-gradient minimization method is adopted to optimize both the electronic and geometrical structures. [94, 95]

For the calculations of the diffusion pathways and the activation energies of adatoms, the constrained $\{N-1\}$-dimensional optimization is performed, where N is the degree of freedom of the unitcell. The schematic diagram illustrating the constrained $\{N-1\}$-dimensional optimization is in Fig. 3.1. To calculate the diffusion pathway and the activation energy between the two metastable structures, a plane ($\{N-1\}$-dimensional (hyper) space; the shaded parallelogram in Fig. 3.1) which is perpendicular to a line connecting the two metastable structures ($\mathbf{r}_1$ and $\mathbf{r}_2$ in Fig. 3.1)

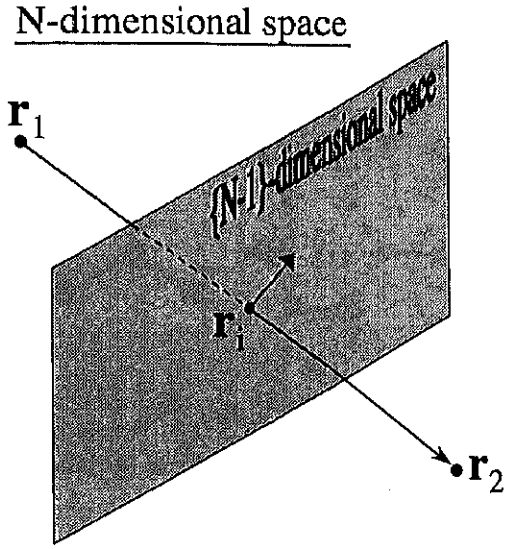

Figure 3.1: The diagram illustrating the constrained $\{N-1\}$-dimensional optimization. The $\mathbf{r}_1$ and $\mathbf{r}_2$ are the points in the N-dimensional (hyper) space, corresponding to metastable structures. The shaded parallelogram indicates the $\{N-1\}$-dimensional (hyper) space perpendicular to a line connecting the $\mathbf{r}_1$ and $\mathbf{r}_2$. The geometrical optimization is performed for the geometry located on the line ($\mathbf{r}_i$) within the $\{N-1\}$-dimensional (hyper) space.

is defined in the N-dimension (hyper) space at first. We perform the geometrical optimization for the geometry located on this line ($\mathbf{r}_i$ in Fig. 3.1) within the $\{N-1\}$-dimensional (hyper) space. The geometrical optimizations are repeated for several geometries located on the line. The results of this constrained optimization yield the intermediate structures of the diffusion process between the two metastable structures.

3.3 Adsorption and Diffusion on the Edge of the Nanotube

The adsorption energies of adatoms on the NT edge and their activation energies of the diffusion on the edge are calculated in this section. The adatom on the NT edge is termed as the "edge adatom" in this thesis. The adsorption energy of the edge adatom E_{rmad} is defined as

$$E_{\rm ad} = \left[E_{\rm tot}^{\rm flat} + N_{\rm ad}E_{\rm atom} - E_{\rm tot}^{\rm adsorb}\right]/N_{\rm ad}, \tag{3.1}$$

where $E_{\rm tot}^{\rm flat}$ is the total energy of the NT without edge adatoms, $E_{\rm atom}$ is an energy of an isolated atom and $N_{\rm ad}$ is the number of the edge adatoms. In this section, $N_{\rm ad}$ varies from 1 to 3. $E_{\rm tot}^{\rm adsorb}$ is the total energy of NT with $N_{\rm ad}$ edge adatoms. The supercell model is used. We use the armchair tube with the length of 4 atomic rows (This tube is termed as the "4-atomic-row armchair tube" in short.) and the 4-atomic-row zigzag tube clusters as the unitcells of the supercell model to calculate the adsorption energies. (See Fig. 3.2.) Bottom atoms of each NT are hydrogenated and fixed during the geometrical optimization to simulate the infinite-length NT. In our LDA calculation, the 3-dimensional periodic boundary condition is imposed. The NT cluster is arranged

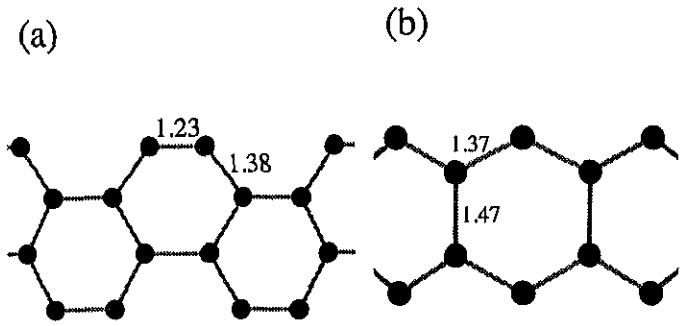

Figure 3.2: Side views of parts of the geometrically optimized structures of the armchair (5,5)-tube edge (a), and the zigzag (9,0)-tube edge (b). The values are bond lengths in Å. Each top row correspond to the NT edges. Bottom atoms are fixed during optimization and hydrogenated. (Hydrogen atoms are not depicted in this figure.)

periodically with sufficiently large separation of 5.3 Å to avoid the inter-tube interactions. The LDA calculations of the large radius NT are time consuming. Hence, we use small radius NT, that is, the (5,5)-tube and the (8,8)-tube for the armchair type and the (9,0)-tube for the zigzag type.

3.3.1 Structures of the edge

Before we calculate the adsorption energies and the activation energies, the structures of the *flat* armchair and zigzag tube edges without adatoms are determined by the LDA calculations. The structures of geometrically optimized edges of the armchair (5,5)-tube and zigzag (9,0)-tube are shown in Fig. 3.2. These figures show parts of the edges of each NT. Each top-row corresponds to the NT edge. The dangling bonds (DBs) on the armchair edge interact with each other, followed by that the bond between the top-row atoms is shortened to be 1.23 Å. This bond length is almost same as that of a carbon triple bond of an acetylene molecule.

On the other hand, The DBs on the top-row atoms of the zigzag NT interact with the second-row atoms. Thus, the bond between the top-row atom and second-row atom is shortened to be 1.37 Å. This bond length is close to that of the double bond of an ethylene molecule. On the other hand, the bond between the second-row atom and the third-row atom is weakened and the bond length becomes 1.47 Å.

3.3.2 Single adatom adsorption and diffusion

We expect that the pentagon, hexagon or heptagon networks are formed on the armchair edge by the adsorption of the several adatoms on the site between the triple bonds of the armchair NT edge (This site is termed as the "seat site" in this thesis.). For example, since the pentagon on the NT edge is a seed of the tube closure, the pentagon network must be eliminated or transformed to the hexagon network to maintain the open edge growth of the NT. Therefore, energetics of adatom adsorption on the NT edge is attractive and important in the open edge growth of the NTs.

In this subsection, we discuss the adsorption of the single adatom. We explore the stable or

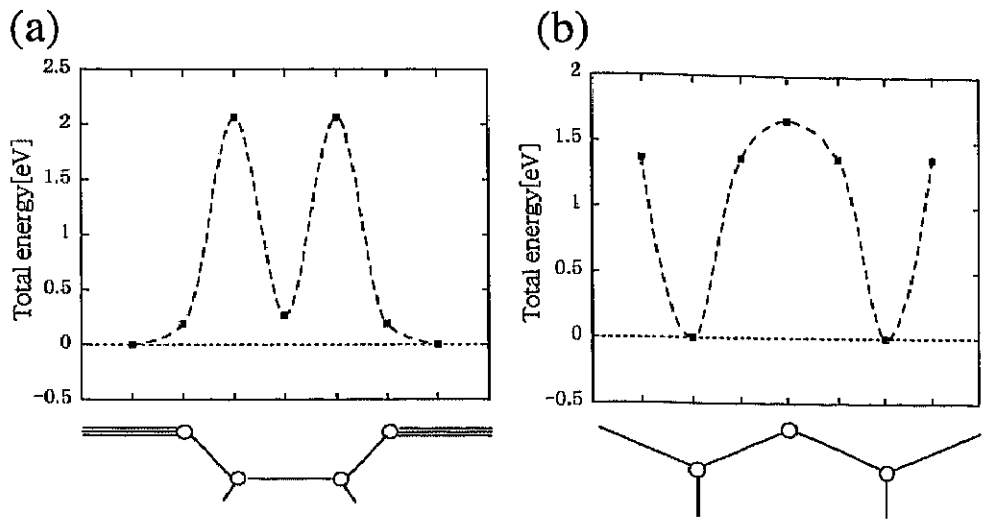

Figure 3.3: The relative total energies of the diffusion of the single adatom along the flat armchair NT edge and the zigzag NT edge are indicated. We calculate the energies at the several points on the edge. The solid squares indicate the energies obtained by our LDA calculations. The dashed lines are only the guides. The edge structures of each tube are also depicted below each plot. (a) The relative total energies of the adsorption on the armchair edge. We set the energy reference (zero energy) as the energy of the adsorption just above the triple bond (arm site). It is found that the activation energy of the diffusion along the flat armchair edge is 2.07 eV. (b) The relative total energies of the adsorption on the zigzag edge. We set the energy reference (zero energy) as the energy of the adsorption just above the second-row atom. It is found that the activation energy of the diffusion along the flat zigzag edge is 1.66 eV.

metastable adsorption sites on the flat armchair (5,5)-tube and the zigzag (9,0)-tube edge. The adatom is placed at a certain site and all the atomic coordinates except for the coordinate of the adatom along the edge are optimized. The relative total energies are plotted in Fig. 3.3 for both the armchair tube (Fig. 3.3 (a)) and the zigzag tube (Fig. 3.3 (b)). We set the energy reference (zero energy) as the energy of the adsorption just above the triple bond (This site is termed as the "arm site" in this thesis.) for the armchair tube. For the zigzag tube, we set the energy reference (zero energy) as the energy of the adsorption just above the second-row atom. The diffusion barrier for the adatom on the armchair edge is the activation energy to migrate from the arm site to the seat site. We obtain the activation energy of 2.07 eV for the (5,5)-tube edge. On the other hand, it is found that the activation energy of the diffusion along the zigzag edge is 1.66 eV.

In the case of the armchair edge, the site just above the triple bond (arm site) is the most stable site for the edge adatom. It is found that the adsorption energy of this arm site is 7.80 eV. On the other hand, the adsorption energy of the seat site is 7.53 eV. The adsorption energy on the site between triple bonds (seat site) is 0.27 eV less than that of the arm site. The adsorption on the seat site is metastable. In the saddle-point structure, the edge adatom is single-coordinated.

The geometrically optimized structures of the adsorption on the arm site and the seat site are depicted in Figs. 3.4 (a) and 3.4 (b). The triangle network is formed when the adatom is adsorbed on the arm site. As a result of the adsorption, the triple bond beneath the adatom is weakened

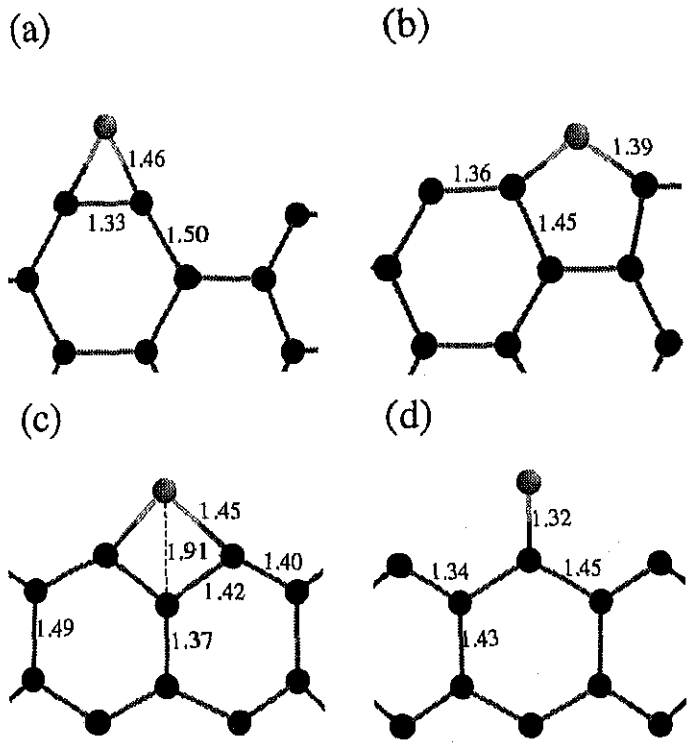

Figure 3.4: Side views of the geometrically optimized structures of the single adatom adsorption on the armchair and zigzag edges are shown. We depict only the edge region around the adatom on the edge. The adatoms are depicted by the lighter spheres. The values in figures are the bond lengths in Å. (a) The adsorption on the arm site of the armchair edge: The triangle network is formed. (b) The adsorption on the seat site of the armchair edge: The pentagon network is formed, which is the metastable structure. (c) The adsorption on the site above the second-row atom of the zigzag edge: The square network is formed. (d) The unstable structure of the single adatom on the zigzag edge. The adatom is single-coordinated.

and the bond length becomes 1.33 Å (Fig. 3.4 (a)). At the seat site, the pentagon network is formed by the adatom adsorption (Fig. 3.4 (b)). In the triangle case, some bond angles are largely distorted from the ideal sp^2 bonding angle. This structure has large distortion energy. From a viewpoint of the bond angle, the pentagon network is more favorable for the carbon atom than the triangle network. But from the DB counting, while the edge adatom on the arm site generates no DB except for the DB on the adatom itself, the edge adatom on the seat site weakens two nearby triple bonds, followed by that the two DBs are generated on the two nearest seat sites of the pentagon network. The adatom, of course, has one DB. In total, there is one (three) DB(s) in the triangle (pentagon) network structure, indicating that the pentagon network is electronically more unfavorable than the triangle network. As a result of the competition between the electronic energy and the lattice distortion energy, the pentagon network has slightly higher energy than the triangle network.

As mentioned above, the pentagon network on the NT edge is responsible to the NT closure.

In addition to the (5,5)-tube, we calculate the adsorption energy of the adsorption of the single adatom on the seat site of the (8,8)-tube edge to investigate the radius dependence of the energies of the pentagon. (The radii of each tube are 3.35 Å for the (5,5)-tube and 5.37 Å for the (8,8)-tube.) The adsorption energies of the single adatom (pentagon network) are 7.53 eV and 7.15 eV for the (5,5)-tube and the (8,8)-tube edges, respectively. It is found that the pentagon is more stable on the smaller radius NT that has high curvature.

In the case of the zigzag edge, the site just above the top-row atom is unstable. As well as the case of the armchair edge, the single-coordinated adatom is unstable on the zigzag edge. The stable site is just above the second-row atom. The edge adatom on this site is bonded to the two top-row atoms and the square network is formed. It is found that the adsorption energy of this site is 9.67 eV, which is larger than that of the arm-site on the armchair edge. This is because the DBs on the top-row atom of the zigzag NT are not stabilized sufficiently.

The geometrically optimized structures are shown in Figs. 3.4 (c) and 3.4 (d). The square network in Fig. 3.4 (c) introduces large distortion into the NT edge. The bonds between the edge adatom and the top-row atom are tilted to the inner side of the NT. The bonds between the top-row atom and the second-row atom nearby the square are weakened and the bond lengths become $1.40 \sim 1.42$ Å because the DBs on the top-row atoms are erased. These bond lengths are close to those of the C—C bond in the benzene molecule and the graphite. On the contrary, since the electrons on the second-row atom are not attracted by the edge atom on which the adatom is adsorbed, the bond between the second-row atom and the third-row atom nearby the square network is reduced to be 1.37 Å. Consequently, the hexagons nearby the square are also distorted. However, because the adatom erases two DBs on the edge, this structure is electronically favorable.

The structure in Fig. 3.4 (d) is unstable. This structure does not induce the large lattice distortion. However, from the viewpoint of the DB, although the adatom erases one DB, the adatom has two DB. The number of the DBs on the zigzag edge is totally increased. Thus, this adsorption structure is electronically unfavorable.

3.3.3 Two-adatom adsorption and diffusion

We discuss in this subsection the adsorption of the two adatoms on the NT edge. Since the open growth is successive formation of the hexagon network, we here focus on the formation and the destruction of the pentagon and the hexagon networks on the NT edge. We have previously found that the pentagon network on the seat site of the armchair edge is energetically favorable. When the additional adatom is placed on the nearest seat site of this pentagon (two adatoms on the edge in total), the two-pentagon array is formed as shown in Fig. 3.5 (b). On the other hand, if the two adatoms are adsorbed simultaneously on the seat site, the hexagon network is formed as shown in Fig. 3.5 (a). We here compare the adsorption energies between the hexagon network and the two-pentagon array for the two adatoms on the edge. Furthermore, to investigate the radius dependence of the energies, the adsorption energies of the two adatoms on the (5,5)-tube and (8,8)-

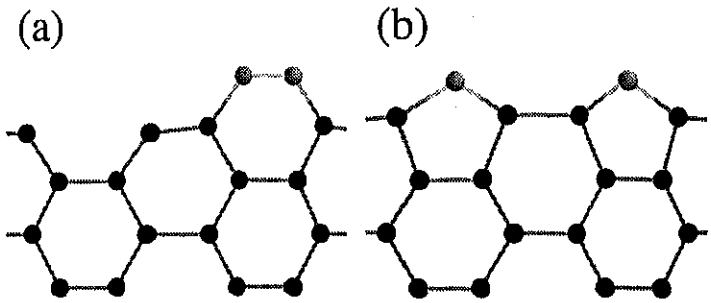

Figure 3.5: Side views of parts of the geometrically optimized structures of the armchair edge with two adatoms. Only top four rows and adatoms are depicted. The adatoms are depicted by the lighter spheres. (a) The hexagon network. (b) The two-pentagon array.

Table 3.1: Relative adsorption energies $E_{\rm ad}$ of two adatoms on the (5,5)-tube and (8,8)-tube edge. We set the energy reference as the energy of the hexagon on the (5,5)-tube. While the two-pentagon array is more favorable on the (5,5)-tube edge than the hexagon network, the hexagon network becomes more favorable than the two-pentagon array on the (8,8)-tube edge.

Tube index	Structure	$E_{\rm ad}$[eV/adatom]
(5,5)	hexagon	0.00
	two-pentagon array	0.02
(8,8)	hexagon	2.42
	two-pentagon array	-0.47

tube edges are calculated. The relative adsorption energies are summarized in Table 3.1. In this Table 3.1, we set the energy reference as the energy of the hexagon on the (5,5)-tube. It is found that the two-pentagon array structure is energetically more favorable than the hexagon network on the (5,5)-tube edge. However, the hexagon becomes energetically favorable on the (8,8)-tube edge. The energy difference between the hexagon network and the two-pentagon array increases with increasing the radius of the NT. The edge of the thin NT with high curvature prefers the two-pentagon array to the hexagon network. Therefore, it is indicated that the thin tube such as the (5,5)-tube is closed more easily than the thick NT during the open edge growth of the NT.

As well as the curvature discussion, the number of DBs on the edge is important factor of the adsorption energetics. The adatom adsorption on the seat site of the armchair edge induces the DBs on the two nearest seat sites since the adatom weakens the triple bonds to be the double bonds. When the two-pentagon array is formed on the armchair edge, there are 4 DBs on the two nearest seat sites and on the two edge adatoms. On the other hand, in the case of the hexagon, the number of DB is two because the bond between the edge adatoms are triple bond. This DB counting indicates that the two-pentagon array is electronically unfavorable.

During the open edge growth, the clean flat edge without adatoms is not always guaranteed and several adatoms are likely to be adsorbed on the NT edge. In the case of the armchair edge, it is expected that several pentagons and hexagons are already formed on the edge.

Here, we assume that the pentagon network has been already formed on the armchair edge. (This pentagon network is termed as the "pre-adsorbed pentagon network".) As mentioned above, the additional adatom is adsorbed on the nearest seat site of the pre-adsorbed pentagon network, followed by that the two-pentagon array is formed. These pentagon networks on the armchair edge must be annealed out to maintain the open edge growth as discussed previously. If the additional adatom on the edge near the pre-adsorbed pentagon network diffuses toward this pentagon network, this pentagon network is likely to be transformed to the hexagon network by incorporation of the additional edge adatom. That is to say, the pentagon network is annealed out and then becomes the hexagon network. Therefore, it is expected that the additional adatom diffusion toward the pre-adsorbed pentagon on the armchair edge is important for the open edge growth.

We calculate the adsorption energies on the several sites near the pre-adsorbed pentagon to investigate the activation energy of this diffusion. We use the (5,5)-tube. The geometrically optimized structures and the relative total energies are shown in Fig. 3.6. Figure 3.6 shows the most probable pathway determined by our LDA calculations from the two-pentagon array geometry (structure A in Fig. 3.6) to a hexagon network on the edge (structure I in Fig. 3.6). As discussed previously, the energy of the two-pentagon array in the structure A in Fig. 3.6 is lower than that of the hexagon network in structure I on the (5,5)-tube. But the energy difference is substantially small. On the edge of the thicker NT, it is expected that the hexagon network becomes more stable than the two-pentagon array. At the structures B~H, we place the an adatom at a certain place along the NT edge and then all the atomic coordinates except for the coordinate of the additional adatom along the NT edge are optimized. It is found that the activation energy to incorporate the additional adatom into the pre-adsorbed pentagon network is 2.29 eV. The adatom starts from the metastable structure A in Fig. 3.6 (a) and approaches the pre-adsorbed pentagon (structures B and C in Fig. 3.6 (a)) with the total energy being increased. At the structures B and C, the additional adatom erases the DB generated by the pre-adsorbed pentagon. After passing through the saddle point (structure C in Fig. 3.6 (a)), the total energy decreases by the bond formation among the additional adatom and two of the pentagon network atoms (structure D in Fig. 3.6 (a)). Then, the adatom is incorporated into the pentagon network spontaneously and the hexagon network is formed (structures E, F, G, H and I in Fig. 3.6 (a)). The activation energy of the diffusion is due to the approach of the additional adatom toward the pre-adsorbed pentagon. Once the additional adatom is bonded to the pre-adsorbed pentagon, the hexagon network spontaneously formed. This surprising findings of spontaneous incorporation is presumably due to the multi-bond formation during the reaction shown in the Fig. 3.6.

This activation energy of 2.29 eV is almost equal to that of the diffusion along the flat armchair edge, suggesting that the additional edge adatom on the nearest seat site of the pre-adsorbed pentagon network diffuses toward the pre-adsorbed pentagon as frequently as the diffusion on the flat edge. Therefore, it is concluded that the pentagon network on the armchair edge can be annealed out by incorporation of the edge adatom. However, this result does not indicate that the

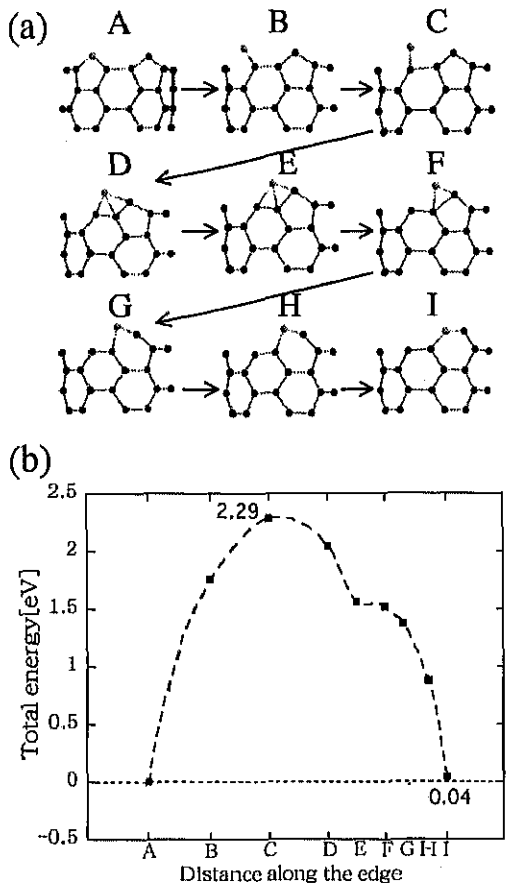

Figure 3.6: (a) Geometrically optimized structures for each site are depicted. The adatoms are depicted by the lighter spheres. At the intermediate structures B~H, all the atomic coordinates except for the coordinate of the additional adatom along the edge are optimized. (b) The relative total energies of the diffusion toward the pre-adsorbed pentagon network. We set the energy reference (zero energy) as the energy of the structure A. The energies obtained by our LDA calculations are indicated by the solid squares. It is found that the activation energy of incorporation of the additional adatom into the pre-adsorbed pentagon network is 2.29 eV.

hexagon network on the armchair edge is formed only by the incorporation of the edge adatom into the pre-adsorbed pentagon network. The other mechanisms, that is, direct incorporation of the gas phase carbon atoms into the pentagon network, the C_2 dimer adsorption on the seat site of the armchair edge and incorporation of the adatom on the NT wall into the pre-adsorbed pentagon, are expected. (We discuss the hexagon formation by incorporation of the adatom on the NT wall in the following section.)

We perform the similar calculations for the diffusion of the adatom on the zigzag edge. The single adatom is placed previously on the zigzag edge. The square network (See Fig. 3.4 (c).) is hereby formed on the zigzag edge. (This square network is termed as the "pre-adsorbed square network".) Since the square network on the zigzag edge also introduces the distortion into the honeycomb lattice of the NT, the square network has to be annealed out to maintain the open

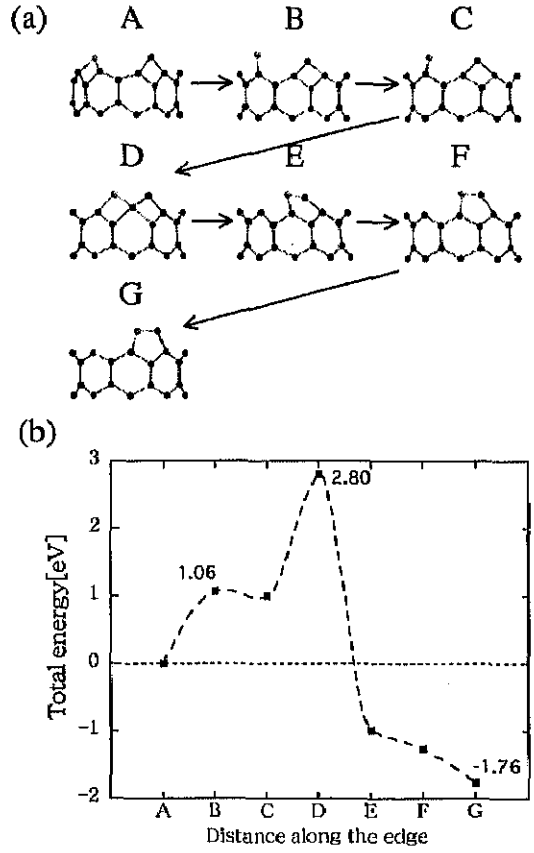

Figure 3.7: (a) Geometrically optimized structures for each site are depicted. The adatoms are depicted by the lighter spheres. At the intermediate structures B∼F, all the atomic coordinates except for the coordinate of the additional adatom along the edge are optimized. (b) The relative energy of the diffusion toward the pre-adsorbed square network. We set the energy reference (zero energy) as the energy of the structure A. The energies obtained by our LDA calculations are indicated by the solid squares. It is found that the activation energy of incorporation of the additional adatom into the pre-adsorbed square network is 2.80 eV.

edge growth of the NT. Hence, we consider the diffusion of the additional edge adatom toward the pre-adsorbed square network on the zigzag edge. We assume that, by incorporation of the additional adatom, the pre-adsorbed square network can be annealed out and then becomes the pentagon network.

We calculate the activation energy to incorporate the additional edge adatom into the pre-adsorbed square network. The additional adatom is placed on the zigzag edge near the pre-adsorbed square network (structure A in Fig. 3.7 (a)) and diffuses toward the pre-adsorbed square network. The pre-adsorbed square network is transformed to the pentagon network (structure G in Fig. 3.7 (a)) by incorporation of the additional adatom. The geometrically optimized structures and the relative total energies are shown in Fig. 3.7. Between the structures B∼F, the additional adatom is placed at a certain place and then all the atomic coordinates except for the coordinate of the additional adatom along the NT edge are optimized. In the structure A in Fig. 3.7 (a), the

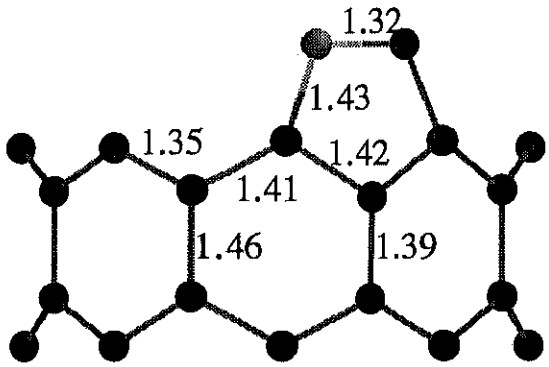

Figure 3.8: We depict the geometrically optimized structures of the pentagon network on the zigzag edge. The values in the figure indicate the bond lengths.

additional adatom is adsorbed on the site just above the second-row atom and two squares are formed on the zigzag edge. In the structure D in Fig. 3.7 (a), the additional adatom is placed on the site just above the second-row atom nearby the pre-adsorbed square network with the result that the two-square array is formed on the zigzag edge. The two-square array introduces the large distortion into the edge and yields the large energy loss. The total energy of this structure is 2.8 eV higher than that of the structure A. The top-row atom to which the two edge adatoms are bonded is largely pulled up by the edge adatoms. Consequently, the hexagon nearby the two squares is extraordinary distorted. When the adatom approaches further the pre-adsorbed square network, the adatom is bonded to two of the square network atoms (structure E in Fig. 3.7 (a)), followed by that the total energy is lowered. After passing through the saddle point (structure D in Fig. 3.7 (a)), the adatom is spontaneously incorporated into the pre-adsorbed square network (structures E, F and G in Fig. 3.7 (a)). As a result, the square network is annealed out and then becomes the pentagon network. The bond lengths of this structure are indicated in Fig. 3.8. The two adatoms on the edge (the pre-adsorbed adatom and the additional adatom) are bonded with the length of 1.32 Å, suggesting that the carbon triple bond is not formed on the top edge of the pentagon. On the other hand, since the edge adatoms erase the DBs on the top-row atoms, the bond between the second-row atom and the third-row atom nearby the pentagon is shortened to be 1.39 Å. It is found that the pentagon is more stable than the two squares on the zigzag edge in the structure A. However, it is also found that the activation energy of the pentagon network formation from the square network plus the additional edge adatom is 2.8 eV. This high activation energy is due to the distorted structure D in Fig. 3.7 (a). It is suggested that the square network is hardly annealed out to pentagon network by the edge diffusion adatom.

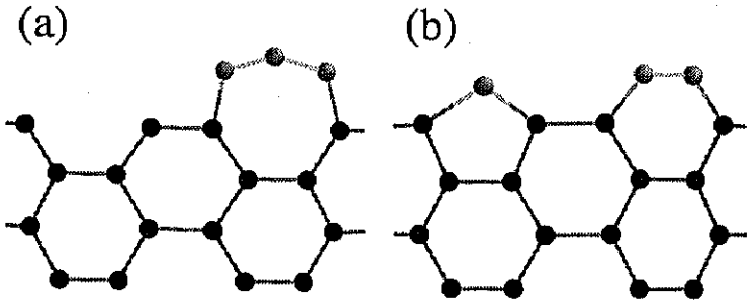

Figure 3.9: Side view of parts of the geometrically optimized structures of the armchair edge with three adatoms. Only top four rows and adatoms are depicted. The adatoms are depicted by the lighter spheres. (a) The heptagon network. (b) The pentagon plus hexagon array.

Table 3.2: Relative adsorption energies $E_{\rm ad}$ of three adatoms on the (5,5)-tube and (8,8)-tube edge. We set the energy reference as the energy of the heptagon on the (5,5)-tube.

Tube index	Structure	$E_{\rm ad}$[eV/adatom]
(5,5)	heptagon	0.00
	hexagon+pentagon	0.76
(8,8)	heptagon	-1.06
	hexagon+pentagon	0.56

3.3.4 Three-adatom adsorption and diffusion

In this subsection, we investigate the three adatoms adsorption on the NT edge. At first, the heptagon network and the pentagon plus hexagon array on the armchair edge are considered. These structures are depicted in Fig. 3.9. The both structures are formed on the (5,5)-tube edge and the (8,8)-tube edge and then the adsorption energies are calculated for each tube. The relative adsorption energies are summarized in Table 3.2. In this Table 3.2, we set the energy reference as the energy of the heptagon on the (5,5)-tube. It is found that the pentagon plus hexagon array (Fig. 3.9 (b)) is more stable than the heptagon network (Fig. 3.9 (a)) on both the (5,5)-tube and the (8,8)-tube edges. The energy difference between the heptagon and the pentagon plus hexagon array increases with increasing the radius of the NT. It is found that the heptagon network that introduces negative curvature to the NT edge is not easily formed on the armchair edge.

The heptagon network formation is also hindrance for the normal open edge growth as well as the pentagon network. If the heptagon network is more stable than the hexagon network on the armchair edge, the hexagon is likely to be transformed to the heptagon by incorporation of one adatom into the hexagon network. The hexagon network on the armchair edge needs to be stable against the decomposition into the pentagon network plus the adatom or the transformation to the heptagon network by incorporation of the adatom to maintain the open edge growth of the NT. In previous subsection, we have obtained the activation energy of 2.25 eV to decompose the

hexagon network into the two-pentagon array. (See Fig. 3.6).

In addition to the decomposition of the hexagon, the transformation from the hexagon network to the heptagon network by incorporation of the additional edge adatom should be considered to discuss the stability of the hexagon network on the armchair edge. Hence, we calculate the activation energy of this transformation by incorporation of the additional adatom into the hexagon network. At first, we prepare the hexagon network on the armchair edge. (This hexagon network is termed as the "pre-adsorbed hexagon network".) Then, the additional adatom is placed on the nearest seat site of the pre-adsorbed hexagon network (This is the pentagon plus hexagon array structure in Fig. 3.9 (b)) and approaches the pre-adsorbed hexagon network. The geometrically optimized structures for each site and the relative total energies are shown in Fig. 3.10. The

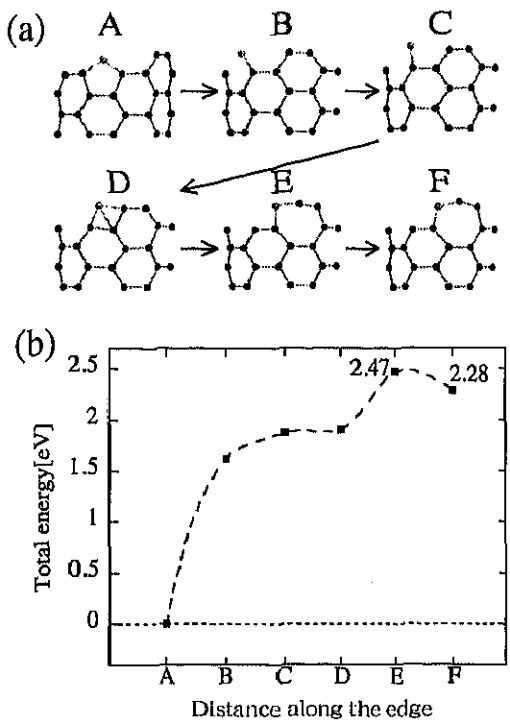

Figure 3.10: (a) Geometrically optimized structures for each site. The additional edge adatoms are depicted by the lighter spheres. At the intermediate steps B~E, all the atomic coordinates except for the coordinate of the additional adatom along the edge are optimized. (b) The relative total energies of the diffusion toward the pre-adsorbed hexagon network. We set the energy reference (zero energy) as the energy of the structure A. The energies obtained by our LDA calculations are indicated by the solid squares. It is found that the activation energy of the incorporation of the additional edge adatom into the pre-adsorbed hexagon network is 2.47eV.

additional adatom diffuses from the initial structure A in Fig. 3.10 toward the pre-adsorbed hexagon network. Finally, the additional adatom is incorporated into the pre-adsorbed hexagon network and the heptagon network is formed (structure F in Fig. 3.10). The bond lengths of the initial structure A and the final structure F are indicated in Fig. 3.11, where the additional adatoms are depicted by the lighter spheres. The additional adatom in Fig. 3.11 (a) is adsorbed on the seat site

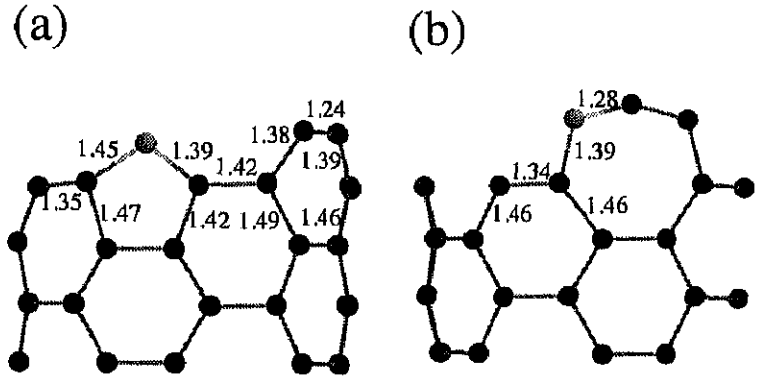

Figure 3.11: We depict the structures of the pentagon and hexagon array and the heptagon network on the armchair edge. The bond lengths in Å are indicated.

with two bonds. The bond lengths are 1.45 Å and 1.39 Å. This difference in the bond lengths is due to the DB generated by the pre-adsorbed hexagon. On the other hand, the heptagon network is depicted in Fig. 3.11 (b). It is found that this heptagon is deformed. (The regular heptagon cannot be formed on the seat site of the armchair edge.) It seems that the region of the seat site is not enough for the three adatoms adsorption. At the intermediate structures B~E, all the atomic coordinates except for the coordinate along the NT edge of the additional adatom are optimized. In the structures B and C, the adatom is bonded to the edge atom with the length of 1.3 Å. The DB generated by the pre-adsorbed hexagon is eliminated by these adsorptions. In these structures, the edge adatom is single-coordinated. In the structure D, the adatom is bonded to one of the pre-adsorbed hexagon network atoms with the length of 1.45 Å, followed by that the triple bond of pre-adsorbed hexagon is weakened to be the double bond. It is found that this bonding does not lower the energy. As the adatom approaches to the pre-adsorbed hexagon further, the additional adatom is incorporated into the pre-adsorbed hexagon network and the heptagon network is formed (structures E and F in Fig. 3.10). The structure E is the saddle-point of this diffusion. We obtain the activation energy of 2.47 eV to transform the hexagon network to the heptagon network on the armchair edge. This activation energy is higher than those of both the edge diffusion on the flat armchair edge and incorporation of the edge adatom into the pentagon network. It is found that the hexagon network is not easily transformed to the heptagon network by incorporation of the edge adatom. In addition, the heptagon network has a high energy on the armchair edge by itself. It should be noted that the energy of the heptagon network is higher than the energies of the structures B and C, where the additional adatom is single-coordinated. On the other hand, if the heptagon is formed on the armchair edge, it is easily decomposed into the pentagon and hexagon networks because of the small activation energy of ~0.2 eV. The heptagon network on the armchair edge is not stable against the decomposition. It is concluded that the heptagon network hardly exists on the armchair edge during the open edge growth of the NT.

We consider the three adatoms adsorption on the zigzag edge in the followings. We prepare the

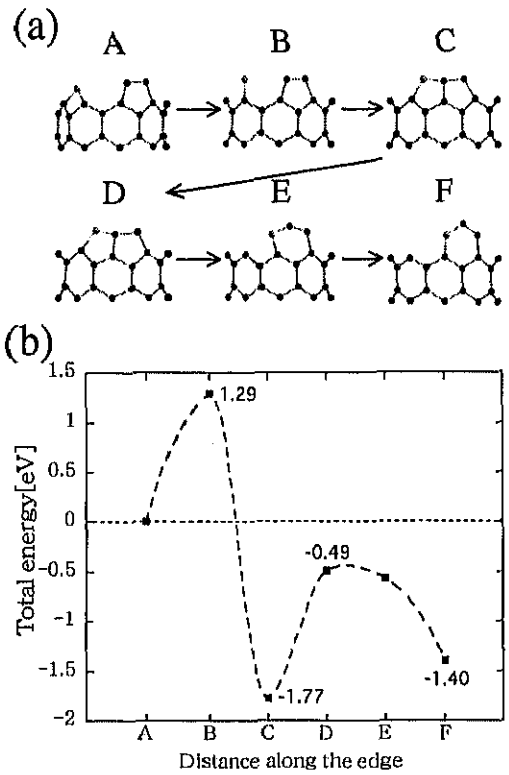

Figure 3.12: (a) Geometrically optimized structures for each site are depicted. The adatoms are depicted by the lighter spheres. At the intermediate structures B~E, all the atomic coordinates except for the coordinate of the additional adatom along the edge are optimized. (b) The relative total energies of the diffusion toward the pre-adsorbed pentagon network. We set the energy reference (zero energy) as the energy of the structure A. The energies obtained by our LDA calculations are indicated by the solid squares. It is found that the activation energy to diffuse from the structure A to the structure C is 1.29 eV and the activation energy to diffuse from structure C to the structure F is 1.28 eV. The former activation energy is due to the saddle-point structure B where the additional adatom is single-coordinated and the latter activation is required incorporate the additional adatom into the pre-adsorbed pentagon network.

pentagon network on the zigzag edge previously. (This pentagon network is termed as the "pre-adsorbed pentagon network".) Then, the additional edge adatom is placed near the pre-adsorbed pentagon and approaches the pre-adsorbed pentagon. It is expected that, by incorporation of the edge adatom, the pre-adsorbed pentagon network is transformed to the hexagon network. We calculate the activation energy of this incorporation. The geometrically optimized structures and the relative total energies are shown in Fig. 3.12. The additional adatom is placed above the second-row atom near the pre-adsorbed pentagon network and the square network is formed near the pre-adsorbed pentagon (structure A in Fig. 3.12 (a)). In the structure C, the additional adatom is bonded to one of the pre-adsorbed pentagon network atoms with the result that the adjacent pentagons network is formed. It is found that the hexagon network is not formed spontaneously from this structure. However, this bonding lowers the total energy. This structure is metastable state on the flat zigzag edge. It is found that the activation energy to form this structure from the

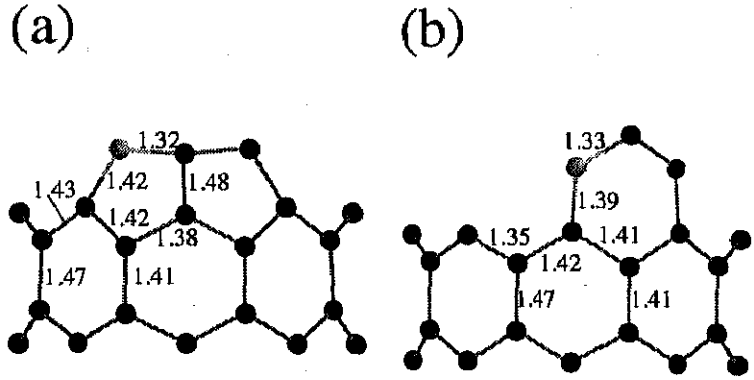

Figure 3.13: We depict the geometrically optimized structures of the adjacent pentagons network (a) and the hexagon network (b) on the zigzag edge. The values in the figures indicate the bond lengths.

structure A is 1.29 eV. This activation energy is due to the saddle-point structure B in Fig. 3.12 (a) where the additional adatom is single-coordinated. The energy of the adjacent pentagons is 1.77 eV lower than that of the square plus pentagon on the zigzag edge (structure A). On the other hand, we obtain the activation energy of 3.06 eV to decompose the adjacent pentagons network into the pentagon network plus the square network on the zigzag edge. Therefore, it is also found that this adjacent pentagons network is sufficiently stable against the decomposition. The bond lengths of this structure are indicated in Fig. 3.13 (a).

As the additional adatom approaches the pre-adsorbed pentagon further, the total energy increases again (structures D and E). The additional adatom is incorporated into the pre-adsorbed pentagon network in the structure E and the hexagon network is formed (structure F). The bond lengths of this structure are also indicated in Fig. 3.13 (b). It is found that the activation energy to form the hexagon network from the adjacent pentagons is 1.28 eV. This activation energy is required to incorporate the additional adatom into the pre-adsorbed pentagon from the structure C.

It should be noted that the energy of the hexagon is higher than that of the adjacent pentagons on the (9,0)-tube edge. Since the (9,0)-tube has large curvature, the adjacent pentagons become more energetically favorable than the hexagon. This fact is similar to that the pentagon networks are energetically favorable than the hexagon on the thin armchair (5,5)-tube. It is found that the trend that the thin tube edge prefer the pentagon holds in both the armchair and zigzag NT. In addition, the higher energy of the hexagon network is probably because this hexagon network is isolated on the zigzag edge. In previous calculation [53], Maiti *et al.* have shown that on the edge of the thin NT, the adjacent pentagons are more stable than the hexagon by the Tersoff-Brenner potential calculation. This calculation has been performed for the stepped edge. Our LDA calculations shows that this tendency holds in the case of the flat edge.

We discuss the number of the DBs of both the adjacent pentagons network and the hexagon network on the zigzag edge. In the case of the hexagon network, the lengths of the bonds between

the edge adatoms are 1.33 Å, indicating that the triple bond is not formed. Therefore, the DB characters remain on these three edge adatoms. On the other hand, the adjacent pentagons network has only two DBs because the one edge adatom is triple-coordinated. It is found that the adjacent pentagons network is also electronically favorable. Therefore, it is expected that the adjacent pentagons network is energetically more favorable than the isolated hexagon network on the flat zigzag edge even in the large radius NT. In the case of the adsorption of the three edge adatoms on the flat zigzag edge, the adjacent pentagons network is likely formed at first. Then, if the additional adatom (4 adatoms on the edge in total) is incorporated into the one of the adjacent pentagons, the adjacent pentagon plus hexagon network is formed. It is expected that the hexagons are formed successively along the edge (the series of the hexagon on the edge) during the growth of the zigzag NT.

3.4 Adsorption and Diffusion on the Wall of the Infinite-Length Nanotube

In the previous section, we consider the adsorption energies and diffusions of the adatoms on the armchair and zigzag NT edge. The NT edge corresponds to the "surface" of the NT. In the open edge growth of the NT, the behavior of the adatom on the NT edge is very important as discussed so far. On the other hand, the carbon adatoms can be adsorbed on the wall of the NT. While there are no DBs on the NT wall, the π orbitals distribute on the NT wall. It should be noted that the adsorption and diffusion of the adatoms on the NT wall are expected to be important even for the open edge growth of the NT, since the wall region is much larger than the edge region. The number of the adatom adsorbed on the NT wall is obviously larger than that of the edge adatoms. If the adatom adsorbed on the NT wall diffuses toward the NT edge, it is probably incorporated into the NT honeycomb lattice at the open edge with the result that the NT continues to grow. Therefore, we discuss the diffusion on the NT wall in this and next section. The adsorption on the NT wall corresponds to the adsorption on the single graphite sheet. At first, we calculate the adsorption energies of the single flat graphite sheet to investigate the effect of the curvature of the NT on the adatom adsorption on the NT wall. In the case of the NT, the adsorption energies are calculated for the infinite-length (5,5)-tube and (9,0)-tube to discuss the diffusion on the NT wall far from the edge. We also perform the calculations of the adsorption on the wall near the NT edge to investigate the effect of the DBs on the edge in the next section.

3.4.1 Flat graphite sheet

For the flat graphite sheet, the sites we used to calculate the adsorption energies are shown in Fig. 3.14, that is, the atom site (A), the bond site (B) and the centre (of the hexagon) site (C). A supercell model is used for calculations. The unitcell consists of the 24-carbon-atom graphite sheet plus a single carbon adatom (25 atoms in total). By using this unitcell, the adatom is sufficiently separated from the other adatoms in the neighboring cells. The periodic boundary condition is

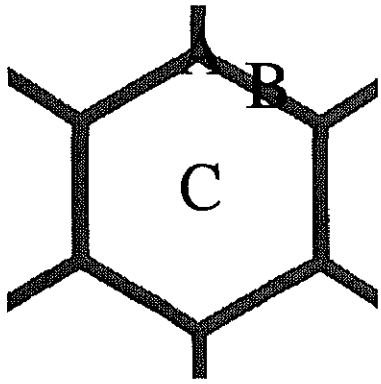

Figure 3.14: Only one hexagon network of the graphite sheet is depicted. Sites of the flat graphite sheet used to calculate the adsorption energy of the adatom are indicated. The A-site is just above the carbon atom of the graphite. (This site is termed as the atom site.) The B-site is above the centre of the graphite C−C bond (the bond site). The C-site is above the centre of the hexagon (the centre site).

imposed to simulate the infinite single graphite sheet. The sufficiently large vacuum region is introduced between the graphite sheets to avoid the inter-layer interaction. The single adatom is initially placed 1.5 Å apart from the graphite sheet at each site and the geometrical optimization is performed. All the atomic coordinates except for the two coordinates of the adatom in the graphite sheet are optimized. The adsorption energies of the A, B and C-sites obtained by our LDA calculations are 2.77 eV, 3.66 eV and 1.52 eV, respectively. The adatom at A-site is bonded to the graphite atom just beneath the adatom with the length of 1.55 Å. The B-site adatom is adsorbed on the graphite atom with two bonds. The lengths of these bonds are 1.49 Å. In the case of C-site, the distance between the adatom and the graphite atom is 2.12 Å at least, suggesting that the interaction between the adatom and the graphite sheet is very weak. Thus, the adsorption energy of this site is small. It is expected that the adatom diffuses along the bonds of the graphite sheet ($\cdots \to A \to B \to A \to \cdots$). The activation energy of this diffusion is 0.89 eV.

3.4.2 Infinite-length nanotubes

The similar calculation is performed for the infinite-length nanotubes. We use the supercell model. The unitcells consist of the 6-atomic-row (5,5)-tube plus a single carbon adatom (61 carbon atoms in total) for the armchair NT and the 8-atomic-row (9,0)-tube plus a single carbon adatom (73 carbon atoms in total) for the zigzag NT. The infinite-length NTs are simulated by the periodic boundary condition along the tubule axis. Each NT is separated from the other NTs in the neighboring cells by sufficiently large vacuum region of 5.3 Å. The LDA calculations for the large radius NTs are time consuming. Further, the adsorption energies on the NT wall are expected to approach that of the flat graphite sheet in the large radius limit. The effects of the curvature on the adatom adsorption on the NT wall are remarkable in the small radius NTs that have high

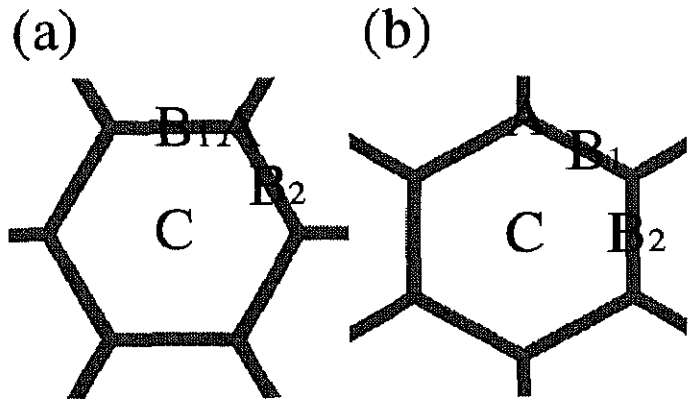

Figure 3.15: Only one hexagon network of the NT is depicted. Sites of the armchair (a) and zigzag (b) tube wall used to calculate the adsorption energy are indicated. Notations of sites are same as the flat graphite sheet The armchair and zigzag tube have two kinds of the bond sites because of the curvature of the NT. In the case of the armchair, one bond (B_2) has the component along the tube axis and the other bond (B_1) has no component along the tube axis. For zigzag, one bond (B_1) has the component along the tube periphery and the other bond (B_2) has no component along the tube periphery. Therefore, the B_1-site and B_2-site are not equivalent for both armchair and zigzag tubes.

Table 3.3: Adsorption energies $E_{\rm ad}$ of the adatom on the wall of armchair or zigzag NT.

Site	$E_{\rm ad}$(armchair) [eV]	$E_{\rm ad}$(zigzag) [eV]
A	3.01	3.20
B_1	4.48	4.66
B_2	3.72	4.31
C	1.22	2.24

curvature. For these reasons, we use the (5,5)-tube and the (9,0)-tube. Figure 3.15 indicates the sites to be considered to calculate the adsorption energies for the armchair and zigzag tubes. The adatom on the NT wall is termed as the "wall adatom" in this thesis. The single adatom is initially placed 1.5 Å apart from the NT wall at each site and all the atomic coordinates except for the coordinates of the wall adatom on the NT wall are optimized. Because of the curvature of the NT, the B_1-site and the B_2-site in Fig. 3.15 are not equivalent for both the armchair and zigzag NTs. The adsorption energies of the adatom on the NT wall obtained by the LDA calculations are summarized in Table 3.3. In the case of the adsorption on the C-site of the armchair NT, the interaction with the NT wall is as weak as that of the flat graphite sheet. On the other hand, since the character of the s-orbital is mixed to the π-orbital on the curved NT wall, the interaction is stronger than that of the flat graphite sheet at A, B_1 and B_2 sites of both the armchair and zigzag NT. In the case of the C-site of the zigzag, the adatom is bonded to the two atoms (the top and bottom atom of a hexagon in Fig. 3.15 (b)) with the lengths of 1.85 Å. Because of the curvature

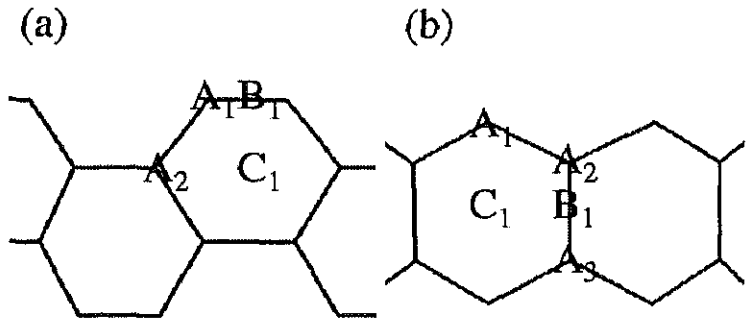

Figure 3.16: Sites of the NT wall near the edge used to calculate the adsorption energy are indicated. Only the top four rows of the armchair tube (a) and the zigzag tube (b) are depicted. The top-rows of each figure correspond to the NT edge. (a) Four sites near the flat armchair edge are considered. (b) Five sites near the flat zigzag edge are considered.

of the NT wall, these two atoms are closer to the adatom than other four atoms of the hexagon. Therefore, the adsorption energy is larger than that of the C-site of the armchair NT. It is expected that the wall adatom also diffuses along the bonds ($\cdots \to B_1 \to A \to B_2 \to A \to B_1 \to \cdots$) with the activation energy of 1.47 (1.46) eV for armchair (zigzag) tube wall. It is found that the activation energy of the diffusion the NT wall is larger than that of the diffusion on the flat graphite sheet. This is because the adsorption energy of the most stable site is increased by the curvature of the NT.

3.5 Adsorption and Diffusion on the Wall near the Nanotube Edge

In the open edge growth of the NT, the adatoms on the NT wall diffusing toward the edge are expected to play an important role in the NT growth. Thus, in addition to the diffusion on the wall of the infinite-length NT, the diffusion on the wall near the NT edge is attractive. The wall adatoms near the edge are affected by the DBs on the edge. We calculate the adsorption energy of the adatom on the NT wall near the NT edge to investigate the effect of the edge on the wall adatom. We use the same supercell model that is used to calculate the adsorption energies of the adatoms on the NT edge in §3.3.

3.5.1 Diffusion on the wall near the flat nanotube edge

In this subsection, the diffusion of the single adatom on the wall near the *flat* NT edge without edge adatoms is considered. The sites we used to calculate the adsorption energies are shown in Fig. 3.16, where the top-rows of each structure correspond to the NT edges. The adatom is initially placed 1.5 Å apart from the NT wall at each site and all the atomic coordinates except for the coordinates of the wall adatom on the NT wall are optimized then.

The adsorption energies of the wall adatom obtained by our LDA calculations are summarized

Table 3.4: Adsorption energies E_{ad} of the adatom on the wall near the NT flat edge.

Site	E_{ad}(armchair) [eV]	E_{ad}(zigzag) [eV]
A_1	5.31	7.67
A_2	3.05	3.53
A_3	-	3.56
B_1	7.01	5.36
C_1	1.29	6.25

in Table 3.4. In the case of the adsorption near the armchair edge, the adatom on the B_1-site is bonded to the two top-row atoms with the length of 1.41 Å. The adatom on the A_1-site is bonded to the top-row atom with the length of 1.32 Å. Because of the DBs on the armchair edge, the adsorption energy of the wall adatom near the edge is larger than that of the adatom on the infinite-length NT wall. Since the adatom on the A_1-site weakens the triple bond between the top-row atoms and generates the DB, the adsorption energy of this site is less than that of the B_1-site. The small adsorption energy of the C_1-site is due to the large distance between the wall adatom and the NT wall (2.24 Å). The wall adatom on the A_2-site is adsorbed on the second-row atom and the adsorption energy is almost equal to the value of the atom site (The A-site in Fig. 3.15 (a). See also Table 3.3.) of the infinite-length NT wall. It is suggested that the effect of the edge turns to be small even at the second-row. This is because the DBs on the armchair edge are stabilized sufficiently by the triple bond formation.

For the case of the zigzag tube, the adsorption energies of the adatom on the wall near the edge are summarized in Table 3.4. Generally speaking, the adsorption energy of the wall adatom near the zigzag edge are larger than those of the wall adatom near the armchair edge. This is due to the DBs which are not stabilized sufficiently on the zigzag edge. The wall adatom on the C_1-site (the centre site of the hexagon) is bonded to the top-row atom. This bond length is 1.36 Å. The wall adatom on the A_1-site forms a strong bond of 1.29 Å with the top-row atom. At the A_2-site, the adatom is adsorbed to the second-row atom with the length of 1.57 Å. Even without wall adatom, the bond between the second-row atom and the third-row atom is relatively weakened (1.47 Å, See Fig. 3.2.). When the adatom is adsorbed just above this bond, that is, the adsorption on the B_1-site, unexpected structure is obtained, which is shown in Fig. 3.17. It is found that the distance between the second-row atom and the third-row atom is extended to 2.09 Å and the corresponding C–C bond is broken. We concentrate on this structure here. If the wall adatom pushes off the second-row atom to the edge, the square network is probably formed on the zigzag edge. (See Fig. 3.4 (c).) Thus, we perform the $\{N-1\}$-dimensional optimization between the structure of the adsorption on the B_1-site and the square network on the zigzag edge to investigate the diffusion pathway and the activation energy. The diffusion pathway and the relative total energies are shown in Fig. 3.18. The structure of the adsorption on the B_1-site is the

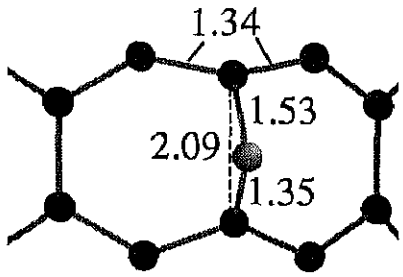

Figure 3.17: The structure of the adsorption on the B_1-site of the zigzag wall near the edge is depicted. We depict only the region around the adatom. Only top four rows and the wall adatom (lighter sphere) are depicted. The values are the bond lengths in Å. The distance between the second-row atom and the third-row atom near by the wall adatom is extended to 2.09 Å and the corresponding C−C bond, which is indicated by the dotted line.

initial structure A in Fig. 3.18 (a). The second-row atom to which the wall adatom (lighter sphere in Fig. 3.18 (a)) is bonded is pushed off by the wall adatom toward the edge and becomes the edge adatom. On the other hand, the wall adatom becomes the second-row atom instead. As a result, the square network is formed on the zigzag edge. (structure E in Fig. 3.18 (a)). The total energy calculation shows that the square network is formed with almost no diffusion barrier. Therefore, it is expected that the square network is spontaneously formed from the structure A. The adatom which is adsorbed on the B_1-site near the zigzag edge does not diffuse to the A_2-site, but rather pushes off the second-row atom, with the result that the wall adatom replaces the second-row atom and the square network is formed simultaneously on the zigzag edge. It is found that the wall adatom can be incorporated into the NT honeycomb lattice and the NT grows. (The square network formation is the first step of the open edge growth.)

As a result of the DB on the zigzag edge, the adsorption energies of the wall adatom near the edge are larger than those of the adatom on the infinite-length zigzag NT wall. It is suggested that the region near the zigzag edge becomes the sink for the wall adatom.

3.5.2 Diffusion on the wall near the armchair edge with the pentagon and hexagon networks

As mentioned previously, it is supposed that the several adatoms are adsorbed on the edge previously (pre-adsorbed edge adatom) during the open edge growth. We investigate the effect of the pre-adsorbed edge adatoms on the armchair edge on the wall adatom in this subsection. The pentagon or hexagon network is formed previously on the armchair edge by the pre-adsorbed edge adatom (the pre-adsorbed pentagon or hexagon network) and the adsorption energies of the wall adatom near the pre-adsorbed pentagon or hexagon networks are calculated then. The sites near the pre-adsorbed pentagon or hexagon used to calculate the adsorption energies are shown in Fig. 3.19. The wall adatom is initially placed 1.5 Å apart from the NT wall at each site and all the

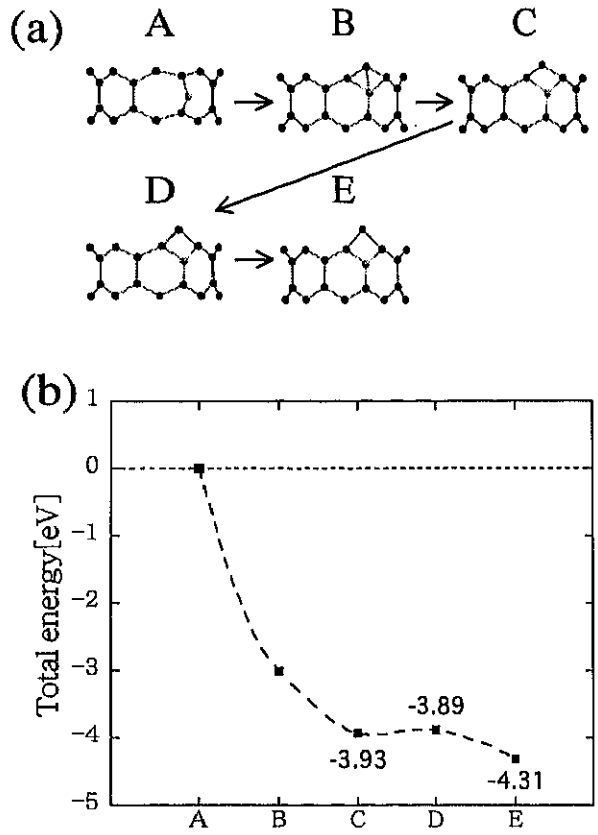

Figure 3.18: (a) Geometrically optimized structures of each site are depicted. The additional wall adatoms are depicted by the lighter spheres. The adatom pushes off the second-layer atom, followed by that the adatom is incorporated into the NT lattice as the second-row atom and the square network is formed on the zigzag edge, simultaneously. (b) The relative total energies of the diffusion of the wall adatom are indicated. We set the energy reference (zero energy) as the energy of the structure A. The energies obtained by our LDA calculations are indicated by the solid squares. Because of the constraint of the wall adatom, the structure A has high energy. It is found that the wall adatom in structure A easily pushes off the second-row atom.

atomic coordinates except for the coordinates of the wall adatom on the NT wall are optimized. The adsorption energies obtained by the LDA calculations are summarized in Table 3.5.

In the case of the adsorption near the pre-adsorbed pentagon network, the adsorption on the B_1-site has the large adsorption energy since the wall adatom erases the DB generated by the pre-adsorbed pentagon. The adsorption on the C_2-site is also affected by this DB. Although, in the case of the flat armchair edge without the pre-adsorbed edge adatom, the adsorption energy of the centre site of the hexagon (C_2-site in Fig. 3.16 (a)) is 1.29 eV, yet the adsorption energy of the centre site of the hexagon nearby the pre-adsorbed pentagon network is 5.40 eV. It is found that the adsorption energy of the NT wall near the DB generated by the pre-adsorbed pentagon network on the armchair edge is larger than that of the adsorption on the wall near the flat armchair edge. The region of the armchair edge around the pre-adsorbed pentagon becomes the sink for the wall adatom. We calculate only the adsorption energy of the typical sites near the pre-adsorbed

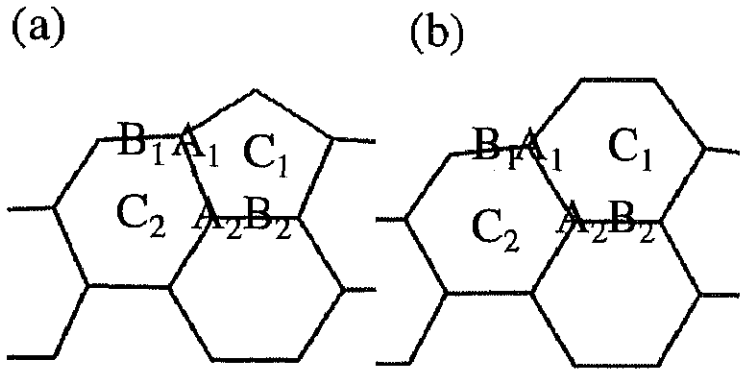

Figure 3.19: Sites of the NT wall near the armchair edge with the pentagon (a) and the hexagon (b) networks used to calculate the adsorption energy are indicated. Only top four rows and the pre-adsorbed pentagon or hexagon network are depicted. The adsorption energies of the adatom on the six sites for each tube are calculated.

Table 3.5: Adsorption energies $E_{\rm ad}$ of the adatom on the armchair NT wall near the edge with the pentagon and hexagon networks.

Site	$E_{\rm ad}$(near pentagon)[eV]	$E_{\rm ad}$(near hexagon)[eV]
A_1	4.53	5.67
A_2	3.92	5.42
B_1	7.28	7.39
B_2	5.63	5.75
C_1	5.49	5.83
C_2	5.40	5.95

pentagon network. If it is assumed that the adatom is likely to diffuse to the sites that have larger adsorption energies, the wall adatom near the pre-adsorbed pentagon network is expected to diffuse $\cdots \rightarrow A_2 \rightarrow C_2 \rightarrow B_1$ or $\cdots \rightarrow A_2 \rightarrow B_2 \rightarrow C_1$.

In § 3.3.3, we conclude that the hexagon network can be formed from the pentagon network on the armchair edge by incorporation of the additional adatom into this pentagon network. As mentioned there, the other mechanisms of the hexagon network formation on the armchair edge can be expected. Hence, we would like to discuss the mechanisms other than the diffusion on the edge to transform the pentagon network to the hexagon network (the pentagon annealing). From the viewpoints of the pentagon annealing and the adatom adsorption on the wall near the pre-adsorbed pentagon network, we should discuss the hexagon network formation by incorporation of the wall adatom into the pentagon network. Therefore, a possibility of the transformation from the structure of the adsorption on the C_1-site to the hexagon network on the armchair edge is investigated. The $\{N-1\}$-dimensional optimization between the structure of the adatom adsorption on the C_1-site and the hexagon network on the armchair edge is performed. The diffusion pathway and the relative total energies are shown in Fig. 3.20. Between the structures C

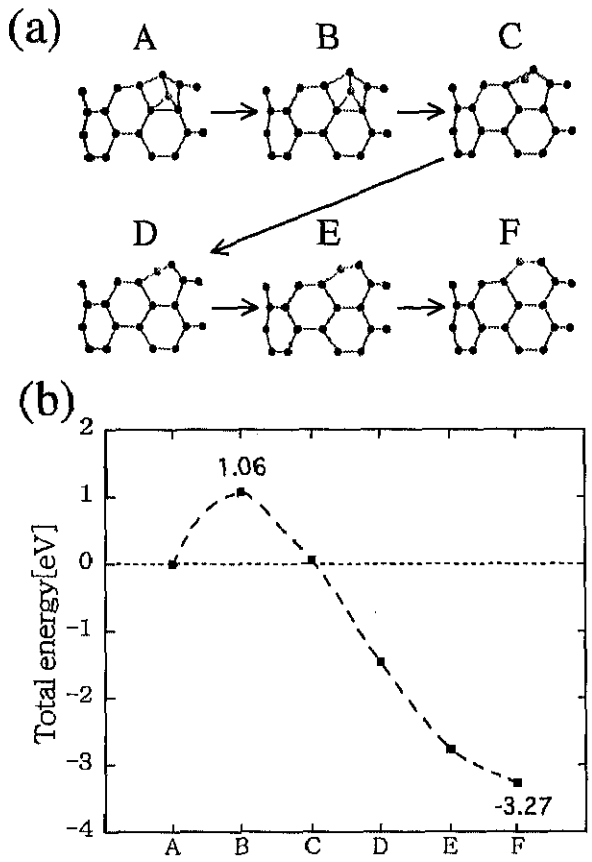

Figure 3.20: (a) Geometrically optimized structures for each site are depicted. The adatoms are depicted by the lighter spheres. This is the probable diffusion pathway of the wall adatom determined by the LDA calculations. (b) The relative total energies of the diffusion of the wall adatom. We set the energy reference (zero energy) as the energy of the structure A. The energies obtained by the LDA calculations are indicated by the solid squares. We obtain the activation energy of 1.06 eV to incorporate the wall adatom into the pre-adsorbed pentagon network.

and D, the pre-adsorbed pentagon incorporates the wall adatom (the lighter sphere in Fig. 3.20) and then becomes the hexagon network. We obtain the activation energy of 1.06 eV to construct the hexagon network on the armchair edge from the pre-adsorbed pentagon network plus the wall adatom. This activation energy is less than that of the transformation by incorporation of the edge adatom into the pentagon network.

In the case of the diffusion on the wall, the wall adatom is always more than double-coordinated and has no deep sink on the NT wall. On the other hand, in the case of the diffusion on the edge, the structure of the saddle point where the edge adatom is single-coordinated has relatively high energy. Furthermore, the stable site such as the seat site nearby the pre-adsorbed pentagon network (Fig. 3.6 (a)A) becomes the deep sink for the edge adatom. Consequently, the activation energy of the diffusion on the edge near the pentagon is relatively large. It is concluded that the wall adatom is incorporated to the pre-adsorbed pentagon more easily than the edge adatom. On the contrary, it is found that the activation energy to decompose the hexagon into the pentagon

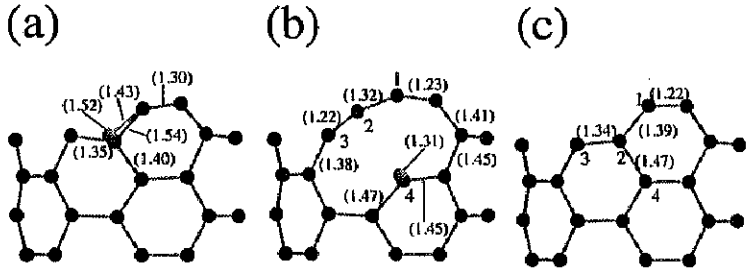

Figure 3.21: Geometrically optimized structures of the adsorption on the A_1-site (a) and adsorption on the A_2-site (b) are depicted. We depicted only the region around the wall adatom. The wall adatoms are indicated by the lighter spheres. The pre-adsorbed hexagon network on the armchair edge without the wall adatom is also depicted in (c). The values in the parentheses are the bond lengths in Å. The numbers of $1 \sim 4$ in (b) and (c) are the atom indexes and correspond with each other. (a) The wall adatom makes the bonds with the top-row atom and one of the pre-adsorbed hexagon network atoms with lengths of 1.52 Å and 1.43 Å, respectively. (b) The adsorption on the A_2-site yields the unexpected structure. The bond between the atom marked as 2 (atom-2) and the atom-4 is broken by the wall adatom adsorption.

network on the NT edge plus the wall adatom is 4.33 eV. This result suggests that the hexagon network formed on the edge is also stable against the decomposition into the pentagon network plus the wall adatom.

We discuss the case of the adsorption on the wall near the pre-adsorbed hexagon on the armchair edge in the followings. The sites used to calculate the adsorption energies are shown in Fig. 3.19 (b). The adsorption on the B_1-site has the large adsorption energy because of the DB on the top-row atom generated by the pre-adsorbed hexagon. The structure of the adsorption on the A_1-site is depicted in Fig. 3.21 (a). The wall adatom is bonded to the top-row atom. Furthermore, the pre-adsorbed hexagon is tilted to form a bond with the wall adatom on the A_1-site. Therefore, this wall adatom is double-coordinated and the adsorption energy is larger than that of the adsorption on the corresponding site near the pre-adsorbed pentagon network on the armchair edge. The remarkable result is obtained in the adsorption on the A_2-site. The structure is depicted in Fig. 3.21 (b). The wall adatom is adsorbed on the atom marked as 4 (atom-4), followed by that the bond between the atom-2 and the atom-4 is broken and the 4-carbon atomic chain is formed. Even in the case of no wall adatom, the bond between the atom-2 and atom-4 is weakened and the bond length becomes 1.47 Å (See Fig. 3.21 (c).) since the DB on the atom-3 attracts the electrons on the atom-2. This mechanism is similar to the case of the flat zigzag edge where the bond between the second-row atom and the third-row atom is weakened by the DBs on the top-row atoms. This atomic chain on the armchair edge is also the hindrance of the open edge growth. However, the following process is one of probable processes to reconstruct the hexagon network on the armchair edge can be considered. We depict the schematic diagram of this probable process in Fig. 3.22. If the bond between the wall adatom and the atom-4 tilts to the NT wall, the wall adatom forms the new bonds with the atom-1 and the atomo-3, with the result that the wall adatom is incorporated

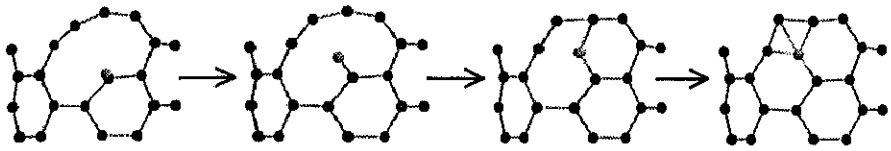

Figure 3.22: The hexagon network reconstruction: When the wall adatom (lighter sphere) is incorporated to the NT lattice as the top-layer atom, the hexagon network on the armchair edge is reconstructed. The final structure corresponds to the hexagon and one edge adatom on the armchair edge.

into the NT lattice. Consequently, the hexagon network is reconstructed. The final structure in Fig. 3.22 corresponds to the hexagon network plus the edge adatom. In the case of the adsorption on the B_2-site, the bond between the atom-2 and atom-4 is not broken, but the length of this bond becomes 1.57 Å. As well as the pentagon network on the armchair edge, the hexagon network also generates the DBs on the nearest seat sites. Therefore, it is found that the hexagon network on the armchair edge provides the deep sinks for the wall adatom.

Because the heptagon formation on the armchair edge is energetically unfavorable as discussed in the § 3.3.4, the transformation of the hexagon to the heptagon by incorporation of the wall adatom is not considered here.

3.5.3 Diffusion on the wall near the zigzag edge with the square and pentagon networks

In this subsection, we consider the adsorption on the NT wall near the zigzag edge with one or two adatoms. The square or pentagon network is previously formed on the zigzag edge (the pre-adsorbed square and pentagon network). Then, the adsorption energies of the wall adatom near the pre-adsorbed square network or pentagon network are calculated. The sites near the pre-adsorbed square and pentagon networks used to calculate the adsorption energies are shown in the Fig. 3.23. The wall adatom is initially placed 1.5 Å apart from the NT wall on each site and all the atomic coordinates except for the coordinates of the wall adatom on the NT wall are optimized. The adsorption energies of each site obtained by our LDA calculations are summarized in Table 3.6.

We discuss the wall adsorption near the pre-adsorbed square network at first. The structure without the wall adatom is already depicted in Fig. 3.4 (c). At the A_1-site and C_1-site, it is found that the adsorption energies are less than those of the corresponding adsorption on the wall near the flat zigzag edge without edge adatoms since the DB on the top-row atom is erased by the pre-adsorbed edge adatom. The structure of the adsorption on the B_1-site is shown in Fig. 3.24 (a). The B_1-site is above the bond between the second-row atom and the third-row atom nearby the pre-adsorbed square. Although this bond is broken by the wall adatom in the case of the flat zigzag edge without edge adatom (Fig. 3.17), yet the corresponding bond nearby the pre-adsorbed square network is not broken by the wall adatom. In the case of no wall adatom, since the edge atom

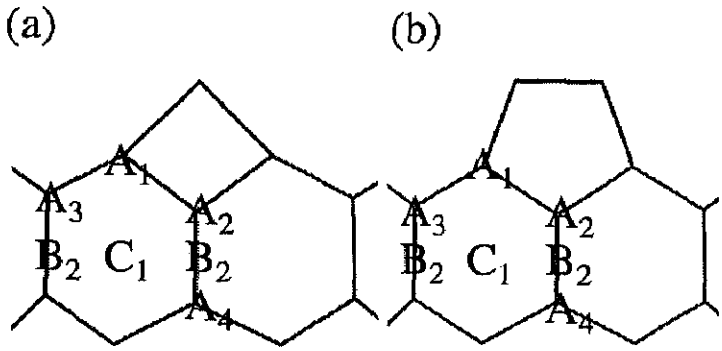

Figure 3.23: Sites on the wall near the zigzag edge with the square (a) and pentagon (b) networks used to calculate the adsorption energies are indicated. Only top four rows and the pre-adsorbed square or pentagon network are depicted. The adsorption energies of the seven sites for each tube are calculated.

Table 3.6: Adsorption energy $E_{\rm ad}$ of the adatom on the zigzag NT wall near the edge with the square and pentagon.

Site	$E_{\rm ad}$(near square)[eV]	$E_{\rm ad}$(near pentagon)[eV]
A_1	5.21	4.39
A_2	5.45	4.00
A_3	3.02	3.22
A_4	4.44	5.45
B_1	5.30	4.87
B_2	5.56	4.84
C_1	2.73	2.71

erase the DB on the top-row atom, this bond is not weakened. (See Fig. 3.4 (c). The bond length is 1.37 Å.) The A_4-site adsorption is above the third-row atom. The wall adatom is bonded to the third-row atom with length of 1.49 Å as shown in Fig. 3.24 (b). This wall adatom also interacts with the second-row atom. The second-row atom is pulled by this wall adatom with the result that the distance between the second-row atom and the wall adatom is shortened to be 1.71 Å. At the B_2-site, the bond just beneath the wall adatom is broken. This structure is shown in Fig. 3.24 (c). As well as the flat zigzag edge, this bond is weakened by the DB on the nearby top-row atom. It is found that the adsorption energies of the sites near the pre-adsorbed square network (A_1, A_2, B_1, C_1 and A_3 sites) are less than those of corresponding sites of the flat zigzag edge without the pre-adsorbed edge adatom. This is because the DBs on the top-row atoms are erased by the pre-adsorbed edge adatom. This effect of the edge adatom on the zigzag edge is opposite to the case of the armchair edge, where the pre-adsorbed edge adatom on the armchair edge generates the DBs and the region around the pre-adsorbed edge adatom provides the deep sink for the wall adatom.

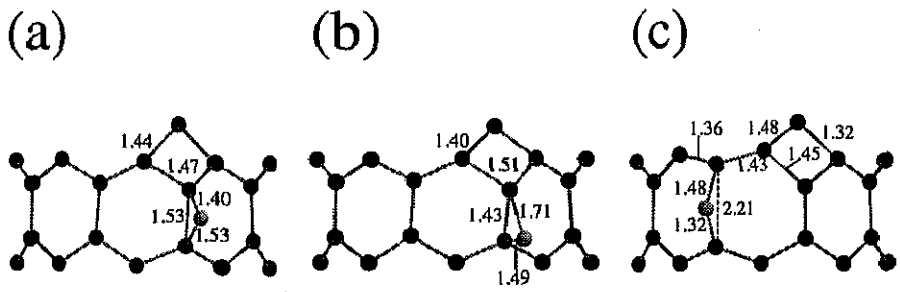

Figure 3.24: Geometrically optimized structures of the adsorption on the wall (B_1, A_4 and B_2 sites) near the pre-adsorbed pentagon network on the zigzag edge are depicted. We depict only the region around the wall adatom. The wall adatoms are indicated by the lighter spheres. The numbers are the bond lengths in Å. (a) The adsorption on the B_1-site. (b) The adsorption on the A_4-site. (c) The adsorption on the B_2-site.

In the § 3.3.3, it is concluded that the square network on the zigzag edge is hardly transformed to the pentagon network by incorporation of the additional edge adatom. Thus, a possibility of the transformation of the square network to the pentagon network by incorporation of the wall adatom is discussed here. We consider only three of the various probable transformation processes. The transformations from the structures of the adsorption on the B_1-site or the B_2-site to the pentagon network on the zigzag edge are assumed. These three processes are depicted in Fig. 3.25. The $\{N-1\}$-dimensional optimization is performed between the B_1-site or the B_2-site adsorption structure and the structure of the pentagon network on the zigzag edge.

In the case of the first process, the wall adatom pushes off the atom marked as 1 (atom-1) to the space between the atom-2 and the atom-3. As a result, the bonds between the atom-2 and the atom-3 (The C_2-C_3 bond. We indicate the bond between the atom-i and the atom-j as the "C_i-C_j bond".) and the C_1-C_4 bond are broken. The new C_1-C_2 bond and the C_1-C_3 bond are formed instead. The wall adatom is bonded to the atom-4. Consequently, the pentagon network is formed on the zigzag edge. The diffusion pathway and the relative total energies of this process are indicated in Fig. 3.26. The atom-1 is pushed off by the wall adatom to the space between the atom-2 and atom-3. At the structure C, the C_2-C_3 bond is broken and the coordination number of the atom-2 changes from 3 to 2. The wall adatom becomes triple-coordinated in structure D. This structure is the saddle-point. At the structure E, the wall adatom is bonded to the atom-4. In addition, the C_1-C_4 bond and the bond between the wall adatom and atom-1 (the C_a-C_1 bond. The subscript "a" indicates the "adatom".) are broken instead, with the result that the pentagon network is constructed. It is found that the activation energy to construct the pentagon network from the square network plus the wall adatom is 1.62 eV.

In the case of the second process, the wall adatom pushes off the atom-1 and the atom-1 pushes off the atom-2 simultaneously, followed by that the wall adatom makes the bond with the atom-4 and the pentagon network is formed. The diffusion pathway and the relative total energies are indicated in Fig. 3.27. Between the structures B and C, the C_1-C_4 bond is broken and the new

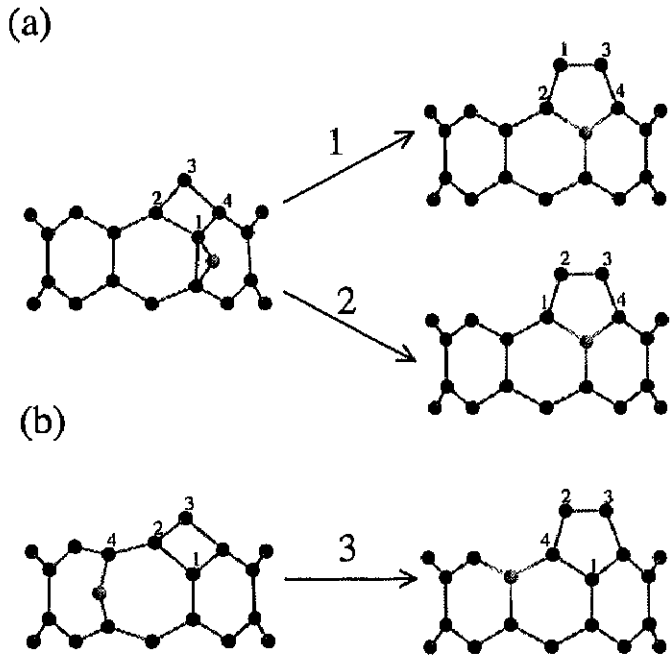

Figure 3.25: The three transformation patterns are indicated. We assume that the pentagon network is constructed from the structure of the adsorption on the B_1-site (a) or the B_2-site (b). The wall adatoms are depicted by the lighter spheres. The numbers near the black spheres are the atom indexes as the guide for the behavior of the atoms. The activation energies are calculated for these three patterns.

C_a-C_4 bond and the C_1-C_3 bond are formed instead. The structure C is largely disordered, yet the adatom and the atom-1~4 are all triple-coordinated and it is expected no DB is generated. Therefore, the activation energy is not increased. The pentagon network is constructed in the structure D. It is found that the activation energy of this process is 0.82 eV.

In the case of the third process, the wall adatom pushes off the atom-2 and the atom-2 pushes off the atom-4 simultaneously. The diffusion pathway and the relative total energies are indicated in Fig. 3.28. At the structure C, the wall adatom become triple-coordinated, with the result that the total energy is lowered. However, the energy is increased again, since the C_1-C_2 bond is broken and the atomic chain (atom-3−atom-2−atom-4) is formed (structures D and E in Fig. 3.28). At the structure F, the pentagon network is constructed by the C_1-C_4 bond formation. It is found that the activation energy of this process is 2.43 eV. In this process, because of the metastable structure C, the relatively large activation is obtained. Among the three processes considered here, the second process is the most probable transformation because of the lowest activation energy.

The three processes of the transformation from the square network plus the wall adatom to the pentagon network are investigated. All the activation energies are less than that of the pentagon network formation on the zigzag edge from the square network plus the edge adatom. It is suggested that the square network on the zigzag edge is transformed to the pentagon network by incorporation

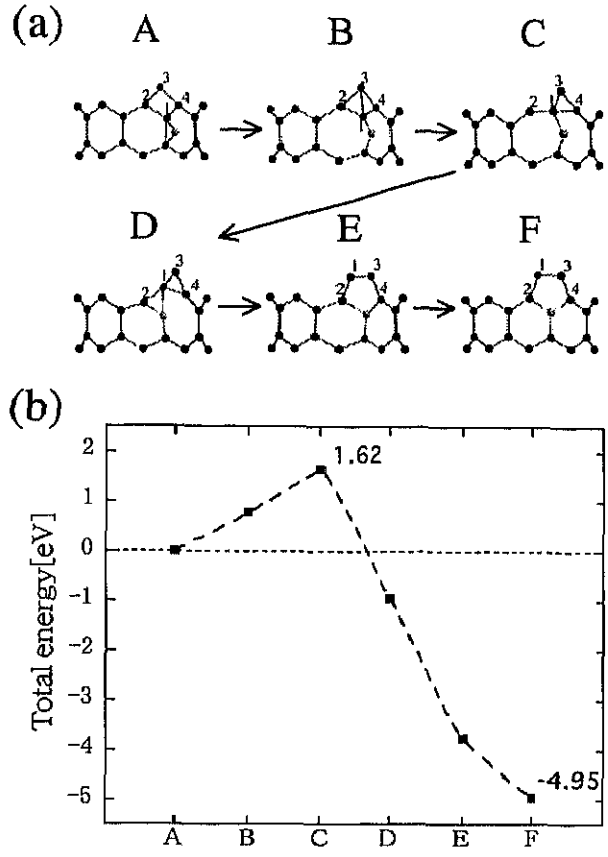

Figure 3.26: The construction of the pentagon network on the zigzag edge from the pre-adsorbed square network plus the wall adatom. (a) The first transformation pathway is indicated. The wall adatoms are depicted by the lighter spheres. The numbers of 1∼4 are the atom indexes to follow the motion of the atoms. In this case, the wall adatom pushes off the atom-1. (b) The relative total energies of the transformation to the pentagon are indicated. We set the energy reference (zero energy) as the energy of the structure A. The energies obtained by our LDA calculations are indicated by the solid squares. In this pentagon network formation process, we obtain the activation energy of 1.62 eV to form the pentagon on the zigzag edge from the pre-adsorbed square network plus the wall adatom. This formation yields the large energy gain of 4.95 eV.

of the wall adatom.

In the following, we discuss the adsorption on the wall near the pre-adsorbed pentagon network on the edge. The results we obtained are similar to the case of the pre-adsorbed square network. The adsorption energies of the A_1-site and the C_1-site are less than those of the flat edge since the pre-adsorbed pentagon erases the DBs on the top-row atoms. At the B_1-site, the bond just beneath the wall adatom is not broken by the wall adatom. This structure is shown in Fig. 3.29 (a). However, this bond is weakened and the bond length becomes 1.52 Å. In the case of the adsorption on the A_4-site, the lattice around the wall adatom is distorted as shown in Fig. 3.29 (b). The second-row atom is pulled and the third-row atom is pushed to inside of the tube by the wall adatom. The wall adatom forms bonds with the second-row atom and the third-row atom with length of 1.46 Å and 1.55 Å, respectively. The wall adatom also interacts with the fourth-row

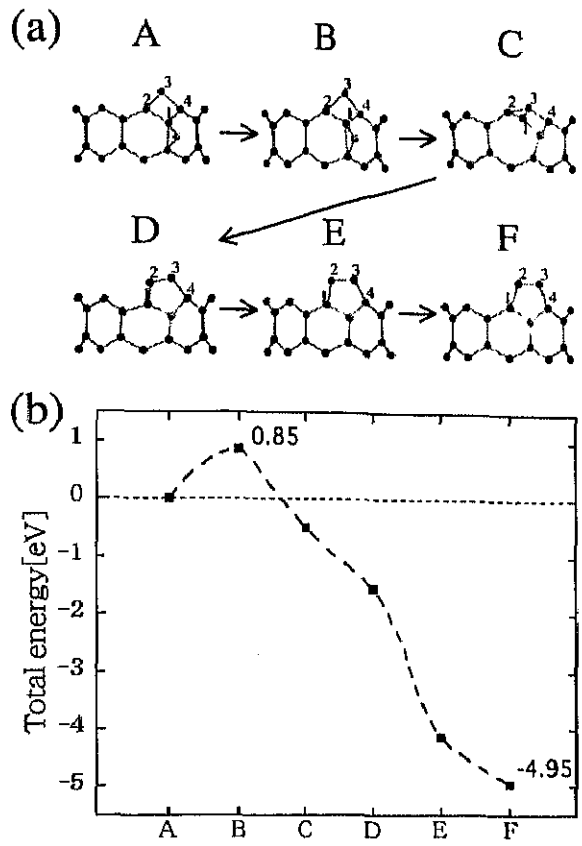

Figure 3.27: The construction of the pentagon network on the zigzag edge from the pre-adsorbed square network plus the wall adatom. (a) The second transformation pathway is indicated. The wall adatoms are depicted by the lighter spheres. The numbers of 1∼4 are the atom indexes to follow the motion of the atoms. In this case, the wall adatom pushes off the atom-1 and the atom-1 pushes off atom-2 simultaneously. (b) The relative total energies of the transformation to the pentagon are indicated. We set the energy reference (zero energy) as the energy of the structure A. The energies obtained by our LDA calculations are indicated by the solid squares. In this pentagon network formation process, we obtain the activation energy of 0.85 eV. This formation yields the large energy gain of 4.95 eV.

atoms. The second-row atom looks like the sp^3 bonding carbon atom. As a result, the adsorption energy of this site is ∼1 eV larger than that of the A_4-site near the pre-adsorbed square network. At the B_2-site, the bond just beneath the wall adatom is also broken. This structure is shown in Fig. 3.29 (c). It is found that the pre-adsorbed pentagon also makes the sink for the wall adatoms shallow because the pre-adsorbed edge adatoms erase the DBs on the top-row atoms.

3.6 Summary

We have presented the adsorption energies and the activation energies of the diffusion of the carbon adatoms on the NT edge and the NT wall. It is found that the pentagon network is more energetically favorable on the edge of the thinner NT. We have also shown that the two-pentagon

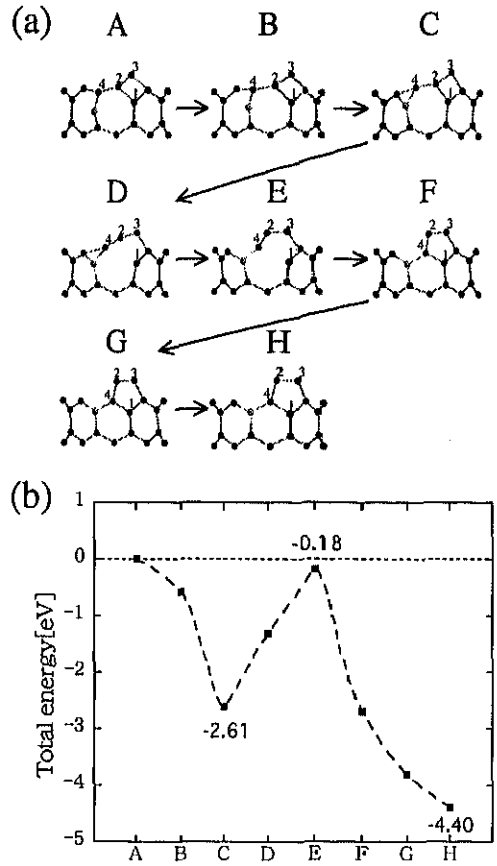

Figure 3.28: The construction of the pentagon network on the zigzag edge from the pre-adsorbed square network plus the wall adatom. (a) The third transformation pathway is indicated. The wall adatoms are depicted by the lighter spheres. The numbers of 1~4 are the atom indexes to follow the motion of the atoms. In this case, the wall adatom pushes off the atom-4 and the atom-1 pushes off atom-4 simultaneously. (b) The relative total energies of the transformation to the pentagon are indicated. We set the energy reference (zero energy) as the energy of the structure A. The energies obtained by our LDA calculations are indicated by the solid squares. In this pentagon network formation process, we obtain the activation energy of 2.43 eV. This activation energy originates in the formation of the pentagon network on the zigzag edge from the metastable structure C.

array is more stable than the hexagon network on the edge of the thin NT such as the (5,5)-tube. These results indicate that the thin NT is easily closed by the pentagons being stable on the edge. Furthermore, it is found that the heptagon network which introduces the negative curvature into the NT honeycomb lattice is energetically unfavorable on the armchair edge.

For the diffusion of the carbon adatom on both the flat armchair and zigzag edge, we have obtained the activation energies of $\sim$ 2 eV. We have also considered the transformation of the polygonal network on the NT edge by incorporation of the additional edge adatom. In the case of the armchair edge, a possibility of the transformation from the pentagon network to the hexagon network (pentagon annealing) has been investigated. We have obtained the activation energy of 2.29 eV for this incorporation, which is almost equal to the activation energy of the diffusion on

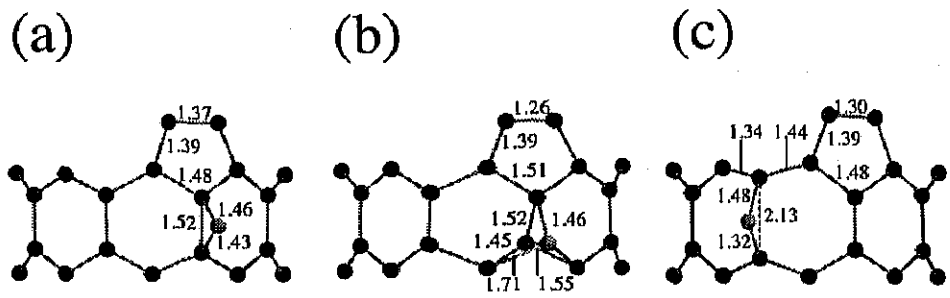

Figure 3.29: Geometrically optimized structures of the adsorption on the wall (B_1, A_4 and B_2 sites) near the pre-adsorbed pentagon network on the zigzag edge are depicted. We depict only the region around the wall adatom. The wall adatoms are indicated by the lighter spheres. The numbers are the bond lengths in Å. (a) The adsorption on the B_1-site. (b) The adsorption on the A_4-site. (c) The adsorption on the B_2-site.

the flat armchair edge. Thus, it is suggested that the pentagon network on the armchair edge can be transformed to the hexagon network by incorporation of the edge adatom. On the other hand, the activation energy of the transformation from the hexagon network to the heptagon network is 2.47 eV. Furthermore, it is found that the heptagon network has large energy on the armchair edge by itself. Therefore, it is expected that the heptagon network is not easily formed on the armchair edge.

In the case of the zigzag edge, the activation energy of edge adatom incorporation into the square network is 2.8 eV. We have obtained the relatively small activation energy of $\sim$ 1.3 eV to incorporate the edge adatom into the hexagon network. However, it is found that the structure of the adjacent pentagons on the zigzag edge is more energetically favorable than the hexagon network on the (9,0)-tube edge. This is because the thin (9,0)-tube has large curvature. Hence, it is concluded that the square and pentagon network on the edge of the thin zigzag NT are hardly annealed by incorporation of the edge adatom.

The diffusion on the NT wall has been also discussed. We have obtained the activation energies of $\sim$ 1.5 eV for the diffusion on both the infinite-length armchair and zigzag NT. It is found that the adsorption energies of the adatom on the NT wall near the flat NT edge are larger than those of the adatom on the infinite-length NT wall because of the DBs on the NT edge. We have presented the adsorption energies of the wall adatom near the pre-adsorbed edge adatoms. In the case of the armchair edge, the pre-adsorbed edge adatom which generates the DBs on the nearest seat sites provides the deep sink for the wall adatoms around the pre-adsorbed edge adatom. On the contrary, in the case of the zigzag edge, the region around the pre-adsorbed edge adatom is not the deep sink for the wall adatom, because the edge adatom erase the DBs on the top-row atoms to which the edge adatom is bonded.

Furthermore, the pentagon network on the armchair edge is transformed to the hexagon network by incorporation of the wall adatom with the activation energy of 1.06 eV. The square network on the zigzag edge is transformed to the pentagon network with the activation energy of 0.82 eV. These

activation energies are less than that of incorporation of the edge adatom. It is suggested that the polygonal defects such as the pentagons and squares networks are annealed out by incorporation of the wall adatoms rather than the edge adatom. Therefore, it is found that the wall adatoms and their diffusion toward the NT edge play the important role in the open edge growth of the NT.

In short, we have discussed in this chapter two kinds of the diffusions, that is, the diffusion on the NT edge and on the NT wall. The former corresponds to the diffusion on the usual material surface. On the other hand, the latter is specific to the NT. It is found that, in the open edge growth mechanisms of the NT, the behavior of the wall adatom near the edge is important as well as the behavior of the edge adatom. This is because the activation energies of incorporation of the wall adatom into the polygonal defects, such as the pentagon network on the armchair edge and the square network on the zigzag edge, are less than those of the edge adatoms.